Lichen Parmotremaperlatum Mediated Greeen Synthesis of Mo Doped CuO Nanoparticles: Photocatalytic Activity and Antibacterial Study

Indramahalakshmi G

mahaan2025@gmail.com

C.P.A. College

Hemaroshini R

C.P.A. College

Kavitha B

C.P.A. College

Research Article

Keywords: Copper Oxide, Amaranth, Photocatalysis, Antibacterial activity, lichen

Posted Date: June 4th, 2024

DOI: https://doi.org/10.21203/rs.3.rs-4431810/v1

Additional Declarations: No competing interests reported.

LICHEN *PARMOTREMAPERLATUM* MEDIATED GREEEN SYNTHESIS OF Mo DOPED CuO NANOPARTICLES: PHOTOCATALYTIC ACTIVITY AND ANTIBACTERIAL STUDY

G. INDRA MAHALAKSHMI*, R. HEMAROSHINI, B. KAVITHA

Department of Chemistry, C.P.A. College, Bodinayakanur-625513, Tamilnadu, India

***Corresponding Author Email.Id: mahaan2025@gmail.com**

Abstract

A "green route" to fabricate nanoparticles has emerged as a revolutionary approach. In this study, CuO, lichen modified CuO (PCuO) and Molybdenum doped lichen extract modified CuO (PCuOM) were successfully synthesized using co-precipitation method. The as-prepared nanoparticles were characterized using UV–visible-diffuse reflectance spectroscopy(UV–vis-DRS), Fourier Transform Infrared Spectroscopy (FT-IR), powder X-ray diffraction (XRD), Scanning Electron Microscopy (SEM) and Energy Dispersive X-ray Spectroscopy (EDS) techniques. The XRD pattern confirms the formation of CuO with JCPDS No.(01-080-1916) and the crystalline nature is found as monoclinic phase of end center. Due to Mo doping and lichen extract activity the PCuOM nanoparticle size was much reduced to14 nm. UV–visible- DRS measurements show a reduction in band gap of PCuOM after dopping with Mo. The FT-IR confirms the presence of functional groups that acts as the capping agent for the synthesis of CuONPs. Mo-CuO nanoparticles showed strong visible-light response and high photocatalytic activity for Amaranth degradation under irradiation by visible-light (400–500 nm). The maximum Amaranth degradation (87%) was achieved with PCuOM concentration of 0.1 g/L, initial Amaranth concentration of 10 μM, pH 7 and irradiation time of 50 min. The antimicrobial activity of all the samples was investigated against both gram positive and gram negative bacteria. The combined effect of phytochemicals and Mo doping shows higher zone of inhibition against *Bacillus subtilus* and *Pseudomonas aeruginosa* about 16 mm and 22 mm respectively, when compared to other bacteria.

Keywords: Copper Oxide, Amaranth, Photocatalysis, Antibacterial activity, lichen

1. Introduction

There has been a tremendous increase in nanotechnology because of its use in biotechnology, chemistry and medicine. Nanotechnology has grown significantly during the last ten years [1-3]. New

avenues in nanoscience, including drug delivery, gene transport, nanomedicine, biosensing etc., have been made possible by advancements in this sector [4,5]. The high surface-to-volume ratio of nanoparticles is one of their distinctive characteristics [6]. Because of atoms on the surface are typically more active than those at the center, this property of nanoparticles makes them more reactive than the bulk material [7,8]. Because of its large surface area, the creation of metal and metal oxide nanoparticles has garnered significant interest in the physical, chemical, biological, medicinal, optical, mechanical and engineering sciences. The intriguing characteristics of metal oxides, including their antibacterial, magnetic, electrical and catalytic activity are caused by their high atom content [9].One can create these nanoparticles via physical, chemical or biological means. Numerous physical and chemical techniques, such as sol-gel synthesis, hydrothermal, laser ablation, lithography etc., call for specialized tools and highly qualified personnel. Additionally, they have harmful impacts on health that are poisonous. Modern scientists have already established a safe, economical and less harmful synthesis approach known as the "biological" or "green" method, which uses plant extract with a small concentration of chemicals to minimize these difficulties.

Many advantages come with this green chemical technique, such as its affordability, suitability for pharmaceutical and biological applications and environmental friendliness.Utilizing environmentally friendly synthesis techniques, the biosynthesis of nanoparticles entails the biological reduction of metals or metal element oxides to their most basic constituents. The shape ranges from 1 to 100 nm, the method has drawn a lot of interest since it is economical and environmentally friendly [10–11].

Lichens are being investigated in great detail for their ability to produce green nanoparticles and for their antimicrobial properties. Lichens are essentially a symbiotic relationship between algae and fungi. They contain several chemicals that are physiologically active [12]. Numerous publications exist regarding the manufacture of nanoparticles derived from various lichen species. Numerous metabolites, including polysaccharides like homo-D-glucan and phenolic chemicals like depside, depsidon and dibenzofurane are found in lichen extracts and may have the ability to function as reducing agents during the creation of nanoparticles. India uses the lichen Parmotremaperlatum, also referred to as black stone flower, as a spice, which are a symbiotic relationship between fungi and algae. It is a member of the Parmeliaceae family of plants. It is a type of perennial lichen that grows on rocks or decaying wood in the temperate Himalayas. They have been utilized as a natural medicine since ancient times and around 700 of their physiologically active constituents have been physically identified. These

constituents are notably distinct from those found in higher plants. Other common names, such as Stone Flower, Shilaapushpa, Kalpasi etc., are presumably a result of its traditional use in Indian medicine's Ayurvedic system for treating ashmari or kidney stones. The powdered medication is used topically on wounds, serves as a good cephalic snuff and enhances digestion. It reduces the production of calculi and tones up the urinary tract. It also keeps the body's temperature normal and suppresses respiratory conditions. The paste of drug is helpful in reducing inflammations. Smoke of drug is believed to relieve headache. It is also used as an important ingredient in cosmetics.

Printing dyes and pigments are among the hazardous pollutants used in the textile industry to produce textile materials and their use is growing daily, making them the most significant threat to human health and the environment, particularly water sources [13–15]. Three types of dye exist: cationic, non-anionic and anionic. Anionic dye is very soluble in water and has an acidic character, making it extremely challenging to extract from water sources [16, 17]. It is less effective to use cleanup methods like microbial degradation or hydrolysis to break down the harmful compounds found in industrial pollutants, such as chlorinated aromatic and aliphatic compounds [18]. In order to regulate these organic pollutants, photocatalytic technology is commonly used [19].

The P-type semi-conducting compound copper oxide (CuO) has a monoclinic structure. Its tiny band gap, excellent thermal conductivity, photovoltaic qualities, high stability and antibacterial activity are just a few of its many fascinating features. CuO has unique characteristics make it useful in a wide range of technological applications, including gas sensors, active catalysts, high-efficiency thermal conductors, magnetic recording media and solar cell applications. Apart from the common characteristics of metal oxide nanostructures like SnO_2, ZnO, WO_3 and TiO_2, CuO nanostructures also possess distinct qualities like super hydrophobicity and magnetic properties [20]. Furthermore, the nanoparticles' excellent photo activity, stability and affordability made them an excellent photocatalyst.

Parmotremaperlatum yields a number of chemicals that have been isolated and named, but no attempt appears to have been made to synthesize CuO NPs. CuO NPs on their own offer many advantages, but bio-functionalized NPs are more potent in the fight against bacteria, viruses and fungi—pathogenic microorganisms. Because biosynthesized CuO NPs made with parmotremaperlatum don't contain any hazardous substances, they are safe to use in medical devices and treatments. Therefore, we are presenting for the first time the biosynthesis of CuO NPs from Parmotremaperlatum in a 50:50 water-ethanol extract and their characterization using techniques such as powder X-ray diffraction (XRD), energy dispersive X-ray spectroscopy (EDS), scanning electron microscopy (SEM), ultraviolet-visible (UV-vis) and Fourier transform infrared (FTIR) spectroscopy. Research has also

been done on their antibacterial efficacy against a few clinical isolates of bacterial pathogens.We investigated the photocatalytic activity of the prepared CuO NPs with Amaranth dye in aqueous solutions as target dyes under visible light irradiation.

2. MATERIALS AND METHODS

2.1. Chemical materials

The analytical grade chemical reagents used in this experiment were purchased from Merck, India. Copper (II) chloride dehydrate ($CuCl_2.2H_2O$), Ammonium heptamolybdatetetrahydrate($(NH_4)_6Mo_7O_{24}.4H_2O$, Sodium hydroxide (NaOH) and double distilled water were used throughout the course of this investigation.

2.2. Plant Materials

The fresh **parmotremaperlatum** lichens were purchesed from market in Bodinayakanur, Theni, Tamilnadu.

2.3. Preparation of lichen extract

Thoroughly dried powder of **parmotremaperlatum** lichens (10 g) were boiled with 100ml of double distilled water at 80°C until volume reduces to half, then cooled. Filtered through Whatman No.1 filter paper (pore size 25 µm) and stored in an air tight container and kept in a refrigerator at 4°C until the completion of the experiment [21].

2.4. Synthesis of CuO nanoparticles

CuO nanoparticles were prepared by dissolving 5 g of $CuCl_2.2H_2O$ in 50 ml of double distilled water. The mixture was kept under constant stirring using a magnetic stirrer at room temperature for 30 minutes. To the above solution 10 ml of *parmotremaperlatum* lichen extract is added dropwise and to the solution 1 equivalence NaOH is added until it reaches optimal pH of 8, then the solution turned to blue on stirring. Subsequently, the stirring was continued for 2 hours at room temperature. Precipitate was filtered using Whatman no.1 filter paper (pore size 25µm) and it was washed with double distilled water to remove the NaOH present in the precipitate. The resulting precipitate was dried at 120°C in a hot air oven. The resultant is the plant extract modified CuO nanoparticles. For the unmodified CuO nanoparticles the same procedure is repeated again without the addition of lichen extract [22].

2.5. Preparation of Mo Doped CuO nanoparticles

Same procedure was repeated for the preparation of lichen extract modified CuO. To this 0.025 equivalence of Ammonium molybdate($(NH_4)_6Mo_7O_{24}.4H_2O$ dissolved in 10 ml of double distilled water was added drop wise into the precipitate of CuO. The pH is adjusted to 8 by adding 1equivalence of NaOH to the above solution. Then the solution turns blue in colour. Precipitate was filtered through WhatmanNo.1 filter paper (pore size 25µm) and it was washed three times with double distilled water to remove excess NaOH present in the precipitate. Then the precipitate was dried in a hot air oven at 120°C for 12 hours. The ash color Mo doped plant extract modified CuO nanoparticles was obtained [23].

2.6. Measurement of photocatalytic activity

Photocatalytic experiments were carried out in an immersion type photoreactor. 300 mL of Amaranth dyewith an initial concentration of 10 µM was taken in a cylindrical glass vessel, which was surrounded by a circulating water jacket to cool the lamp. Air was bubbled continuously into the aliquot by an air bump in order to provide a constant source of dissolved oxygen. Before light irradiation the reaction mixture was stirred in dark for 15 min to achieve the adsorption-desorption equilibrium between the catalyst and dye molecules. A 300 W Xe arc lamp with an ultraviolet cut off filter was used as the visible light irradiation source. During the course of light irradiation, 5 mL of aliquot was collected at regular time interval of 10 min. Then the samples were centrifuged to remove the photocatalyst and the filtrate was analysed by UV – visible spectrometer at λ_{max} = 514 nm. The photodegradation of Amaranth dye was calculated by the formula given below:

$$\boldsymbol{Photodegradation}\ (\%) = \frac{\boldsymbol{C_0 - C}}{\boldsymbol{C_0}}\ \boldsymbol{x\ 100} \qquad \textbf{(1)}$$

Where, C_0 is the concentration of Amaranth dye before irradiation time and C is the concentration of Amaranth dyeafter a certain irradiation time.

2.7. Antibacterial Test

The antibacterial activity of synthesized CuO, Plant modified CuO and Mo doped plant modified CuO nanoparticles was tested against bacteria by zone inhibition disc diffusion method. These nanoparticles were investigated against Gram +ve and Gram -ve strains like Bacillus subtilis, Salmonella and pseudomonas aeruginosa that were cultured on agar plates added with same concentration of CuO, PCuO and PCuOM nanoparticles. The nutrient agar medium for the growth ofbacteria was prepared by dissolving 2.8 g of agarin 100 ml ofdistilled water in a conical flask and

sterilized in an autoclave at 121°C for 15 min. The warm agar nutrient was poured into the sterilized Petridish, inoculated with the microorganism and allowed to dry in the air. The sample to be tested was added then incubated at 37 °C for 24 hours and the diameter of the inhibition zone was measured.

3. RESULTS AND DISCUSSION

3.1. UV-vis-DRS spectroscopy

The UV-vis-DRS spectroscopy is most widely used technique to investigate the optical properties of the particles. The analysis was done in the range of 200-800 nm. The solid UV-vis-DRS spectra of CuO, lichen modified CuO, (PCuO) and Molybdenum doped lichen extract modified CuO, (PCuOM) nanoparticles are represented in the Fig. 1 (a). UV absorption spectra shows a decrease in absorbance with an increase in wavelength. It was found that after modification with Lichen extract the resulting PCuO nanoparticles exhibited a strong absorption band at 400 nm i.e., (Red shifted) than that of pure CuO 371 nm. Mo doped lichen modified CuO nanoparticles PCuOM showed absorption at 378 nm.

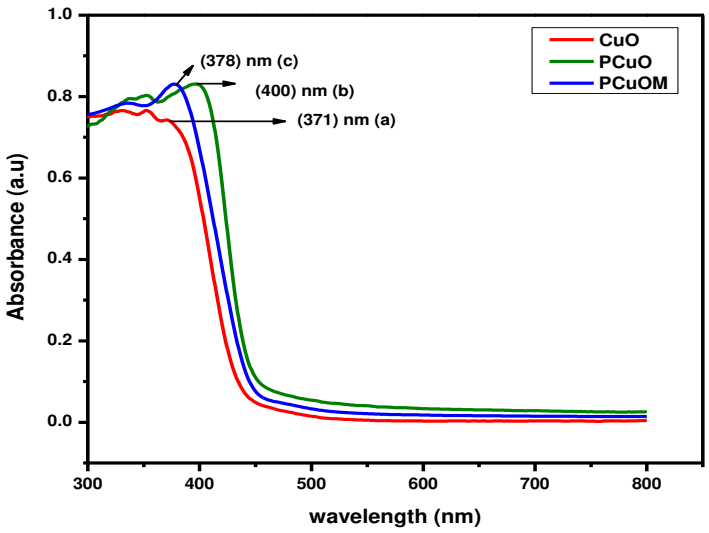

Fig. 1(a) Absorbance wavelength of CuO, PCuO and PCuOM nanoparticles

The Tauc plot is used to calculate the energy band gap of above synthesized nanoparticles i.e., the band gaps are calculated by slope intercept manipulation from the graphs between $(\alpha h\nu)^2$ and hν (eV) [24]:

$$\alpha h\upsilon = K\,(h\upsilon - Eg)^n \qquad (2)$$

Where, α = absorption coefficient,hυ = energy of the incident photon, K= proportionality constant and Eg = band gap energy, while, n=2 for direct band gap & n= ½ for indirect band gap [25]. The band gap energy was calculated from the absorption spectra. Extrapolation of the linear part until its linear part until its intersection with the hυ axis provided the values of the band gap shown in the Fig. 1 (b), (c) and (d). The calculated band gap of samples of CuO, PCuO and PCuOM nanoparticles is 2.83 eV, 2.74 eV and 2.76 eV respectively. Lichen extract and the Mo doping reduces the band gap of CuO.

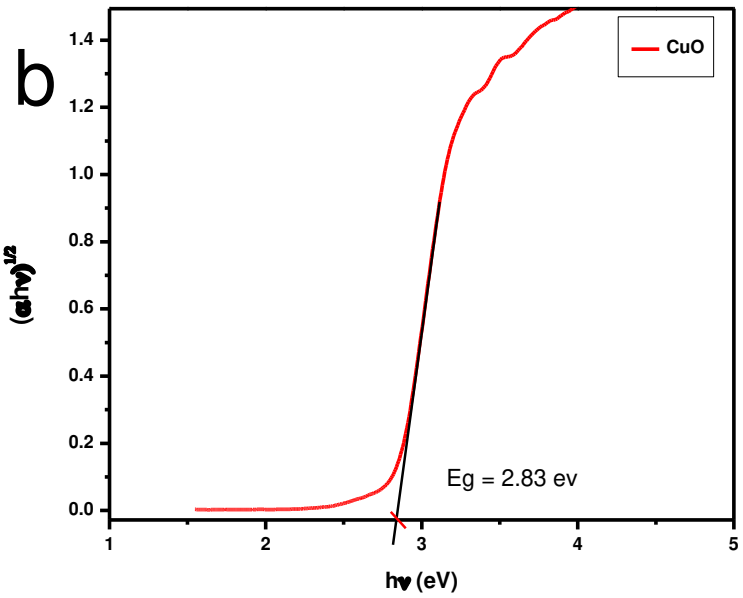

Fig. 1 (b) Tauc plot of CuO

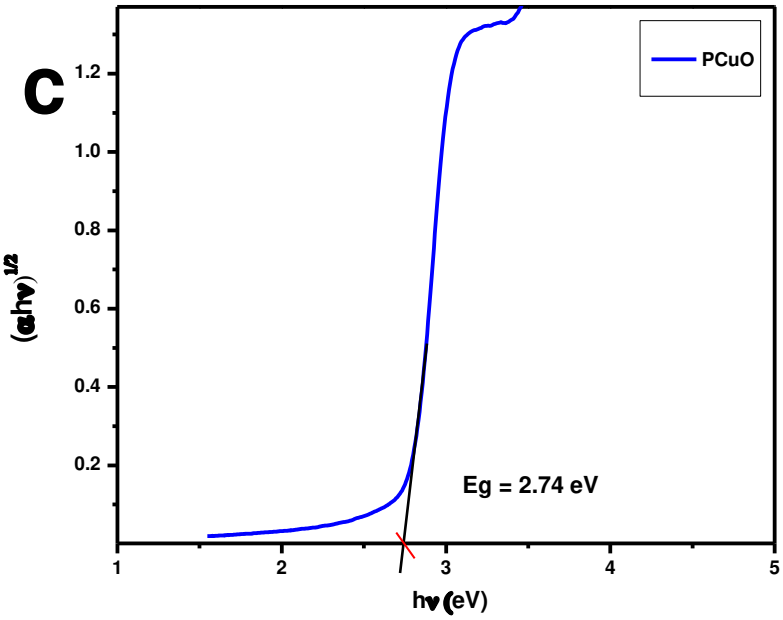

Fig. 1 (c) Tauc plot of PCuO

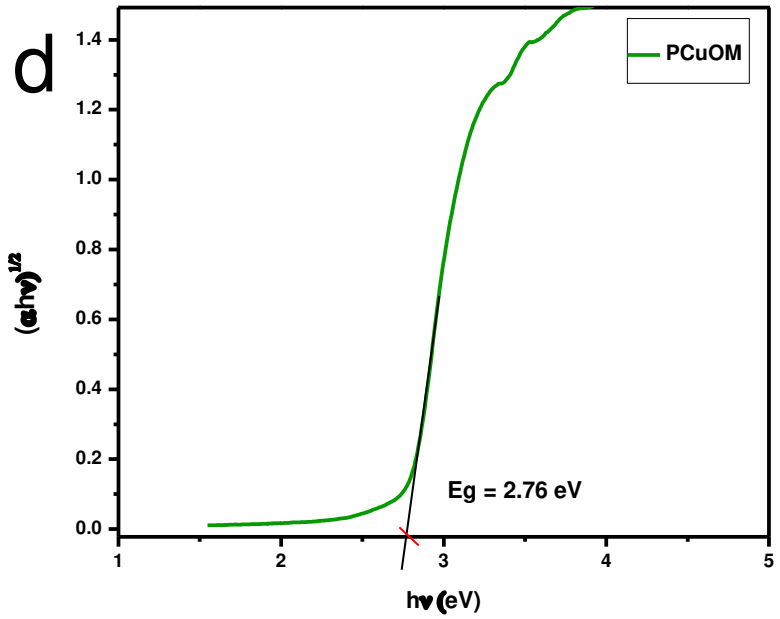

Fig. 1 (d) Tauc plot of PCuOM

3.2. X-ray diffraction spectroscopy (XRD)

XRD was a rapid analytical technique primarily used for phase identification of a crystallite material and can provide information on unit cell dimensions. The average crystalline size was calculated using Debye Scherrer's formula:

$$D = k\lambda/\beta\cos\theta \qquad (3)$$

Where, D is the crystalline size, λ is the wavelength (1.5406A° for Cu Kα) of the X-ray radiation, β is the full width at half maximum of the peaks at the diffracting angle θ [26]. The average crystalline size wascalculated. According to JCPDS data (01-080-1916),the exhibited diffraction peaks at 2θ = 32.18° (1 1 0), 35.26° (-1 1 1), 38.54° (1 1 1), 47.10° (-1 1 2), 48.47° (-20 2), 53.34° (0 2 0) , 57.93° (2 0 2), 61.35º (-1 1 3), 65.94 (1 1 3) and 67.98 (2 2 0) corresponds to the different planes of monoclinic phase-end centered of CuO and PCuO nanoparticles and the diffraction peaks at 38.31º (2 0 0), 65.74º (0 2 2) and 67.90 (-3 1 1) corresponds to different planes of molybdenum nanoparticles with JCPDS data (00-041-0254) PCuO and PCuOM. XRD peaks are broad in comparison with that of CuO, which shows that the lichen extract and Molybdenum nanoparticles inhibited the crystallization of CuO. These result shows that smaller particles grow more easily when incorporated with metal ions and the phytochemicals of lichen. The XRD for synthesized CuO, PCuO and PCuOM are shown in Fig. 2. The average crystalline size was found to be 24 nm, 13 nm and 14 nm for CuO, PCuO and PCuOM respectively.

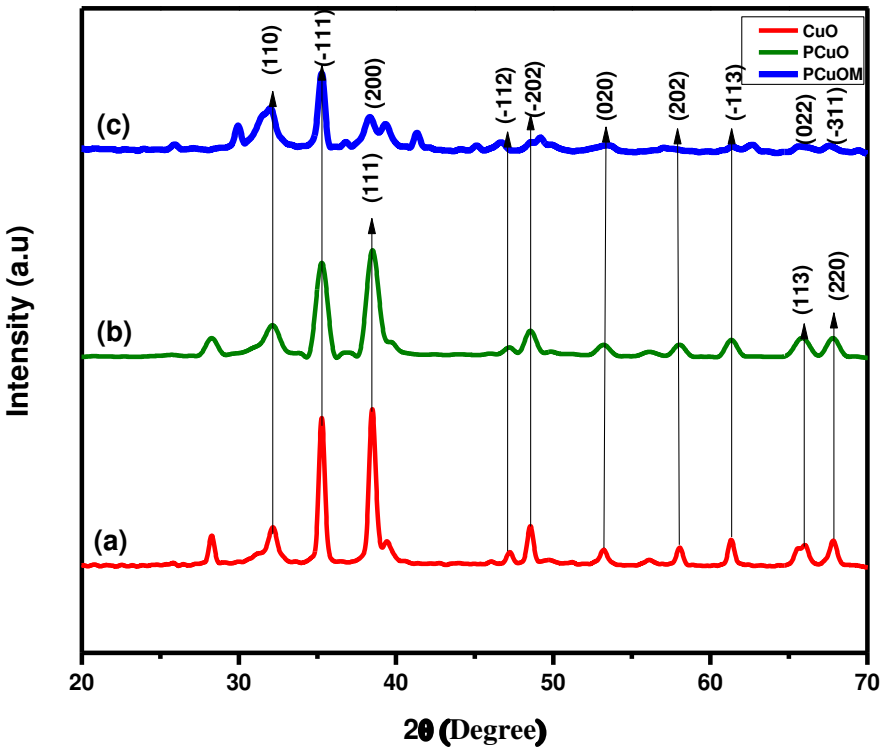

Fig. 2. XRD pattern of CuO, PCuO and PCuOM

3.3. FT-IR spectroscopy

FT-IR spectroscopy is useful in measuring the absorption of IR radiations by a sample and the results were shown by means of a wavelength. The FTIR spectrum of CuO, PCuO and PCuOM nanoparticles was shown in Fig. 3. It can be resolved that the secondary metabolites of *permutaperlatum* lichen extract can act as a strong capping agent during the synthesis of CuO nanoparticles are shown in (Table-1).The extended band at 3200–3600 cm^{-1} is related to the hydroxyl (OH) stretching vibration of the physically adsorbed water molecules from atmosphere. Strong peaks at 655,646, 664 cm^{-1} confirmed the formation of monoclinic CuO phases [27]. Sharp bands observed at 1032 and 1024 cm^{-1} due to C-N stretching vibration of aromatic and aliphatic amine.The peak at 1410 cm^{-1}shows the presence of –COO carboxylic acid. The weak peak absorbed at 872 cm^{-1} shows the presence of Mo=O [28], peak intensity is less than that of Cu-O which shows that the Mo doping is very less in CuO. The obtained FT-IR analysis of CuO, PCuO and PCuOM nanoparticles were attributed by the phytochemicals like flavonoids and terpenoids in the Parmotremaperlatum lichen extract.

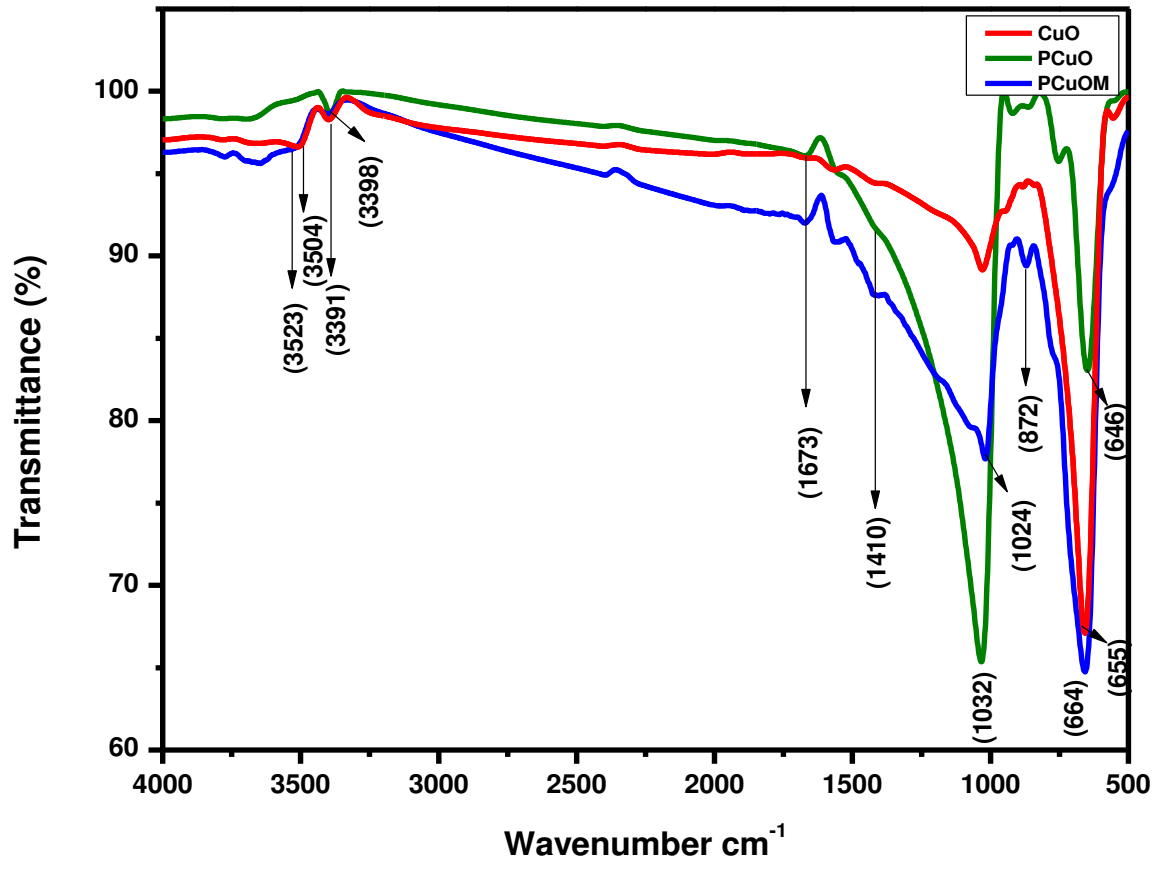

Fig. 3. FT-IR Spectrum of CuO, PCuO and PCuOM nanoparticles

Table. 1. IR vibrational spectrum assignments for CuO, PCuO and PCuOM nanoparticles

Wavenumber (cm^{-1})			IR vibrational assignment
CuO	**PCuO**	**PCuOM**	
3504 3391	3398	3523 3391	O-H stretching of water molecules
-	1673	1673	C=O stretching

-	1410	1410	Asymmetric bending of ($-CH_2$)
-	1032	1024	C-N stretching vibration of aromatic and aliphatic amine
655	646	664	Cu-O stretching
-	-	872	Mo=O stretching

3.4. SEM and EDX Spectroscopy

Scanning Electron Microscope (SEM) was carried out to study the morphology of CuO. Fig.4(a-c) shows the SEM images of CuO, PCuO and PCuOM nanoparticles. The irregular nanoparticles of CuO revealed by SEM is due to Vanderwaals force that pull the particles together. This occurs mostly in nanoparticles of smaller sizes. Furthermore examination of SEM images of PCuO and PCuOM shows that decreases in particle size due to the addition of secondary metabolites found. In lichen extract, this confirms the presence of alkaloids, terpenoids, flavonoids, tannins and aminoacids. On doping with Mo irregular rock like structure with agglomerates are observed.

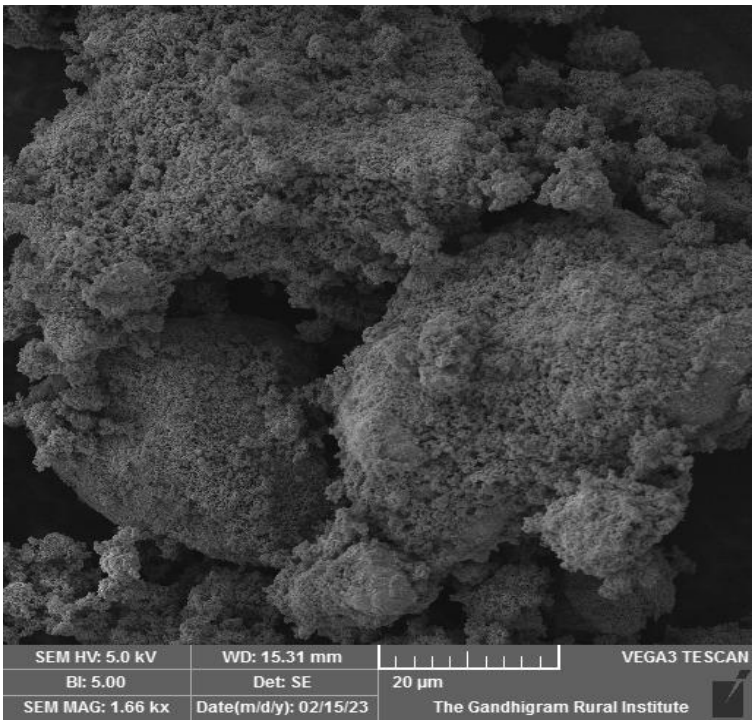

Fig. 4 (a) SEM image of CuO

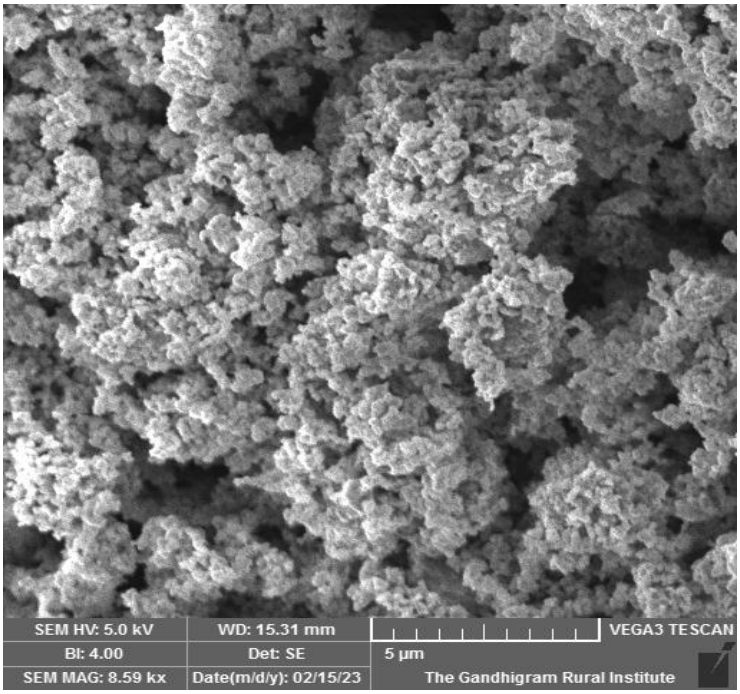

Fig. 4 (b) SEM image of PCuO

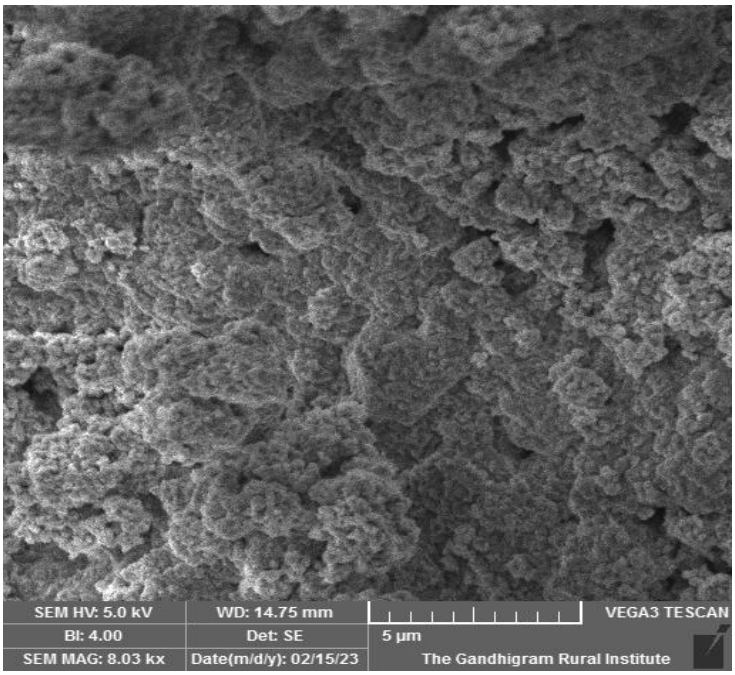

Fig. 4(c) SEM image of PCuOM

EDX analysis revealed the purity of CuO, PCuO and PCuOM nanoparticles (Fig. 5 (a), (b) and (c)). Oxygen and Copperin EDX spectrum indicate the copperin the form of oxide.The weight compositions for Copper (Cu) and oxygen (O) in CuO, PCuO and PCuOM were 77.17%, 45.72%, 64.21% and 22.83% ,43.05%, 22.15% and Molybdenum (Mo) in doping were 0.62% respectively shown in (Table-2).Carbon and Nitrogen were also detected in small amount owing to interactions with phytochemicals present in the lichen extract.

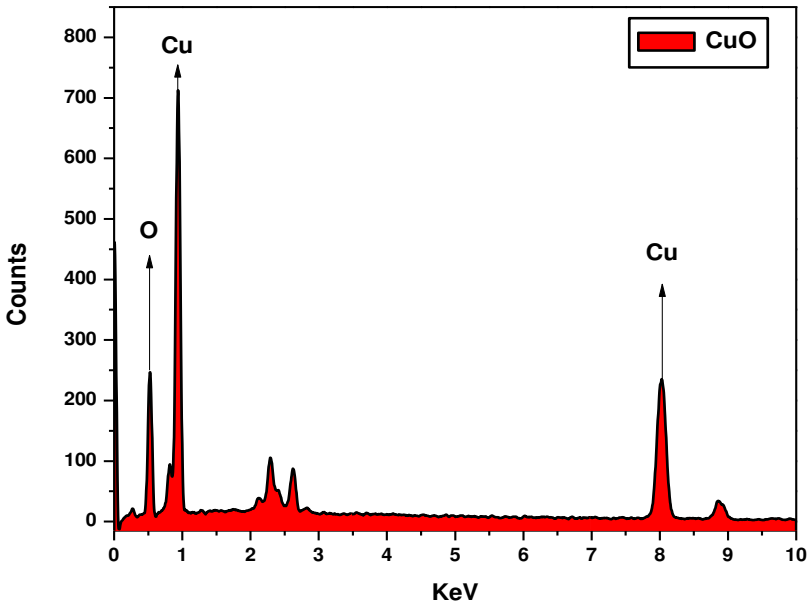

Fig. 5 (a) EDAX Spectrum of CuO

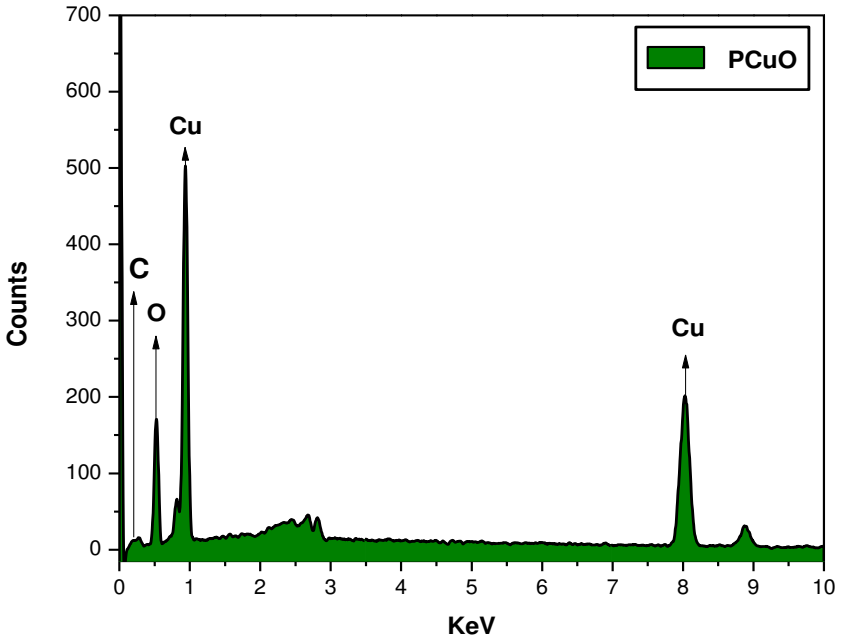

Fig. 5 (b) EDAX Spectrum of PCuO

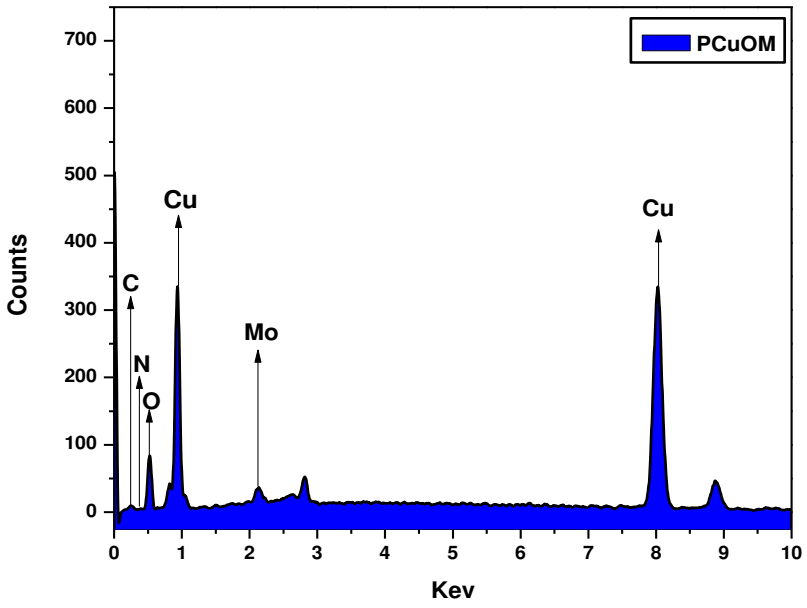

Fig. 5 (c) EDAX Spectrum of PCuOM

Table 2. Elemental composition of CuO, PCuO and PCuOM

S.NO.	Sample	Atomic %	KeV
1.	CuO	Cu=77.17 O=22.83	Cu= 8 KeV O=0.5 KeV
2.	PCuO	Cu= 45.72 O=43.05 C=11.23	Cu= 8 KeV O=0.5 KeV
3.	PCuOM	Cu= 64.21 O=22.15 C=10.22 N= 2.8 Mo= 0.62	Cu= 8 KeV O=0.5 KeV Mo= 2.321 kev

3.5 Photocatalytic activity

The photocatalytic activity of the prepared nanoparticles were investigated by degradation of Amaranth (10 μM) dye under visible light radiation. The catalyst concentration was fixed at 0.1 g/L and photodegradation of Amaranth was monitored by change in absorbance (λ_{max}= 514 nm) as a function of irradiation time. Fig. 6 (a) shows the change in absorption spectra of Amaranthdye using PCuOM nanoparticles.

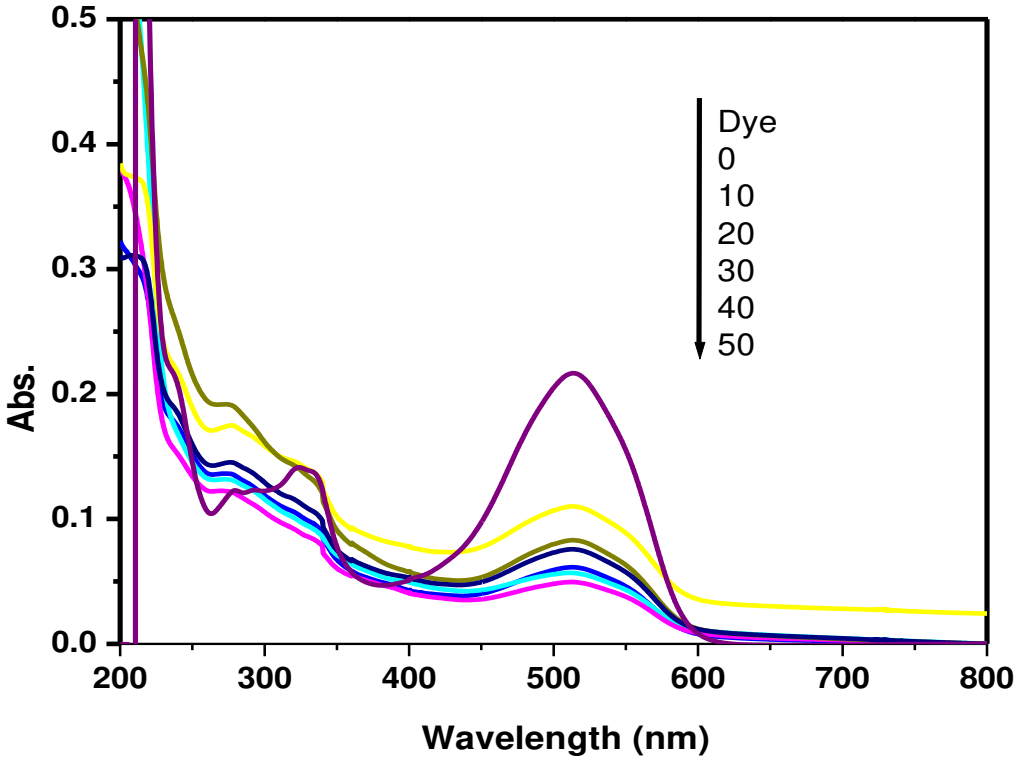

Fig. 6 (a) The time dependent UV-visible spectral changes of Amaranthdye using PCuOM under visible light irradiation

It is noticed that the absorption intensity of Amaranthdye decreases gradually with increasing of irradiation time. The decrease in absorbance in the UV-region demonstrates the degradation of aromatic structure. PCuOM shows higher photocatalytic activity (87 %). Photodegradation percentage of PCuOM, PCuO,CuO and without catalyst was shown in Fig.6 (b).

In order to obtain quantitative information of the photocatalytic activity of the as-prepared products, the kinetics of photocatalytic degradation of Amaranthdye was also investigated [29, 30]. The degradation of Amaranthdye can be described using the pseudo first-order kinetic model as shown below.

$$-\ln \frac{C}{C_0} = kt \qquad (4)$$

Where, k is the first-order apparent rate constant and t is the light irradiation time. C_0 and C_t represent the concentrations of Amaranthdye at beginning and time t, respectively. Fig.6 (c) shows the kinetic plot of photodegradation curves of Amaranthdye using PCuOM, PCuO, CuO and without catalyst. The value of the apparent rate constant k and the correlation coefficient R^2 are shown in Fig. 6 (c). The rate constant of PCuOM, PCuO, CuO and without catalyst is 6.2 x 10^{-3} min^{-1}, 8.6 x 10^{-3} min^{-1}, 1.91 x 10^{-2} $min^{-1}$and 2.22 x 10^{-2} min^{-1}respectively.

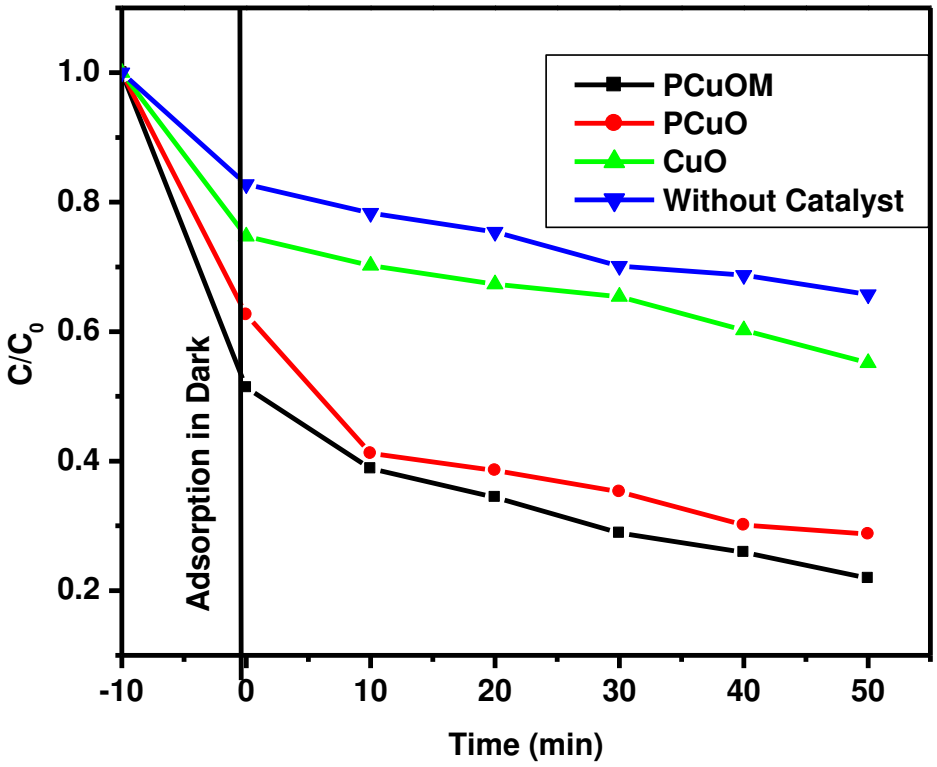

Fig. 6 (b) Photodegradation of Amaranth dye in the presence of PCuOM, PCuO, CuO and without catalyst

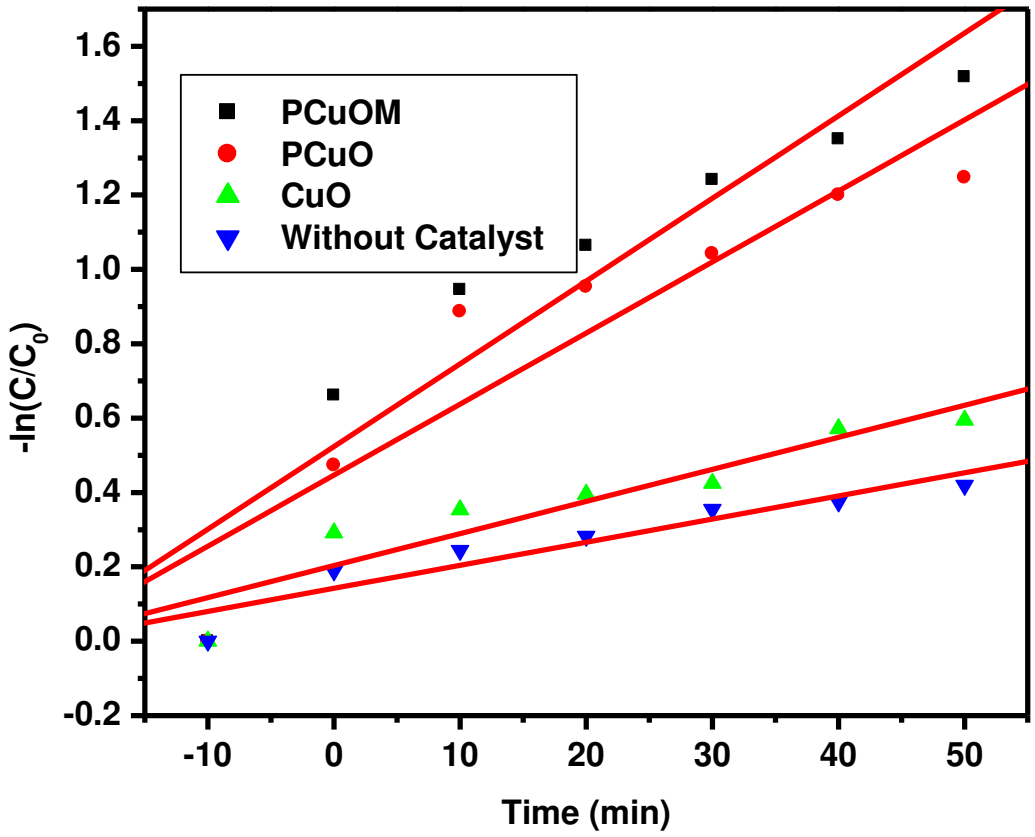

Fig. 6 (c) Kinetics of photodegradation of Amaranth dye in the presence of PCuOM, PCuO, CuO and without catalyst

3.6. Antibacterial Test

The antibacterial activity of the CuO , PCuO and PCuOM nanomaterial was determined by using well diffusion method against Gram positive and Gram negative bacteria: *Staphyloccocusaureus, Bacillus subtilus* (gram positive) and *Salmonella, Pseudomonas aeruginosa* (gram negative) are shown in Fig. 7 (a, b, c and d) were tested at same concentration. The variation in the sensitivity or resistance to both gram positive and gram negative bacterial populations might be due to the differences in the cell structure, physiology, metabolism or degree of contact oforganisms with nanoparticles. At biological pH values, the overall charge of bacterial cells was negative due to the additional carboxylic groups present in the lipoproteins on the bacterial surface which upon dissociation makes the makes the cell surface negative·

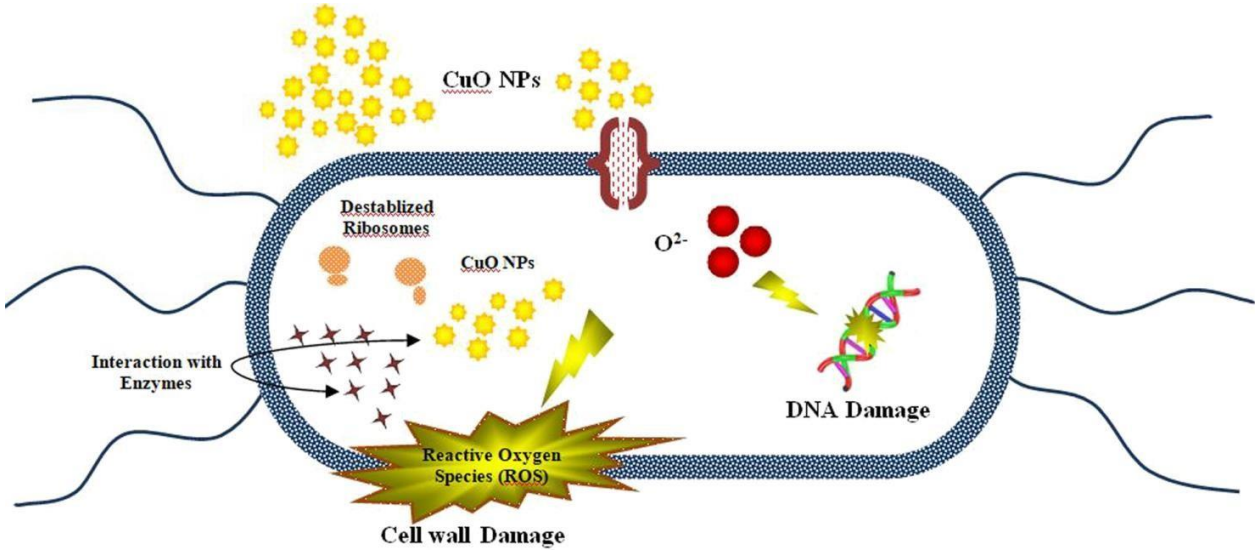

.

Fig. 7.Mechanism of PCuOM nanoparticles against bacteria

The obtained zone of inhibition rate of CuO, lichen modified CuO (PCuO) and Mo doped CuO (PCuOM) nanoparticles against *Staphyloccocusaureusis, Bacillus subtilus, Salmonella and Pseudomonas aeruginosa* are given in Table-3. The variation in the inhibition rate as shown in Fig. 7 may be due to the difference in the cell wall structure. Smaller sized particles can effectively interact with bacterial membranes due to their large surface area, thus enhancing their antibacterial efficiency. PCuO and PCuOM nanoparticles show excellent antibacterial activity then pure CuO, which is due to the effect of secondary metabolites of lichen extract and Molybdenum doping. The combined effect of phytochemicals and Mo doping shows higher zone of inhibition against *Bacillus subtilus* and *Pseudomonas aeruginosa* about 16 mm and 22 mm respectively, when compared to other bacteria.

Table. 3. The antimicrobial activity of CuO, PCuO and PCuOM nanoparticles

Tested Bacteria	Gram Reaction	Sample inhibition zone (mm)		
		CuO	PCuO	PCuOM
Staphyloccocusaureus	+ ve	9	11	13
Bacillus subtilus	+ ve	10	14	16
Salmonella	-ve	13	17	17
Pseudomonas aeruginosa	-ve	16	21	22

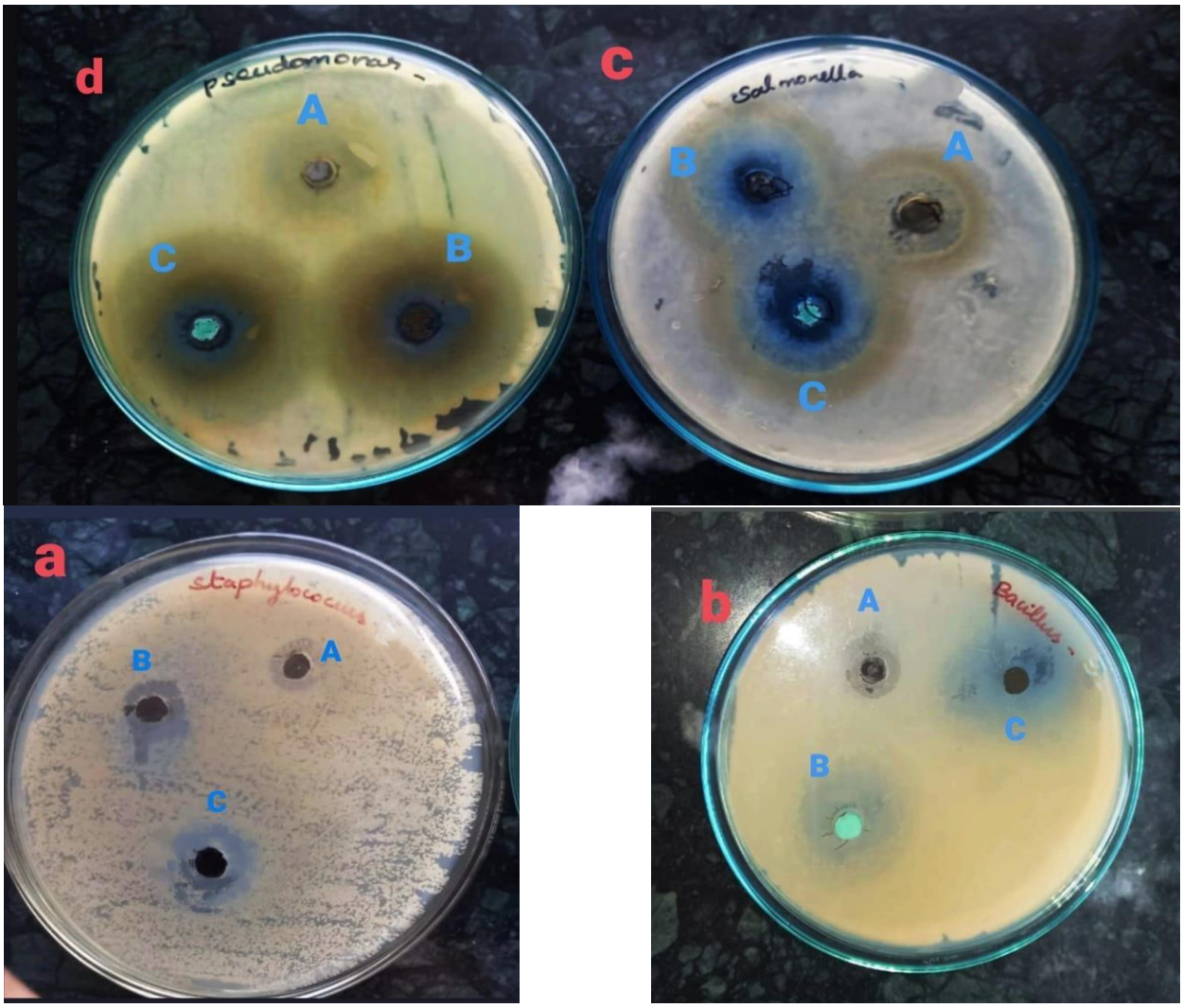

Fig. 3.5. CuO, PCuO and PCuOM nanoparticles against (a) *S. aureus* , (b) *Bacillus Subtilus*, (c) *Salmonella* and (d) *Pseudomonas aeruginosa*.

4. CONCLUSION

In this study, CuO, lichen modified CuO (PCuO) and Molybdenum doped lichen extract modified CuO (PCuOM) were successfully synthesized using co-precipitation method. From the obtained UV-vis-DRS spectroscopy the λmax value is red shifted from UV to visible region so it can be used in direct sunlight thus it is used in photocatalytic and solar cell applications. The band gap is reduced to 2.74 eV for PCuO than that of CuO, which implifies that lesser activation energy is required for the synthesis, so the energy consumption is low. FT-IR spectrum confirms the metal oxide and various functional groups of phytochemicals present in the lichen extract of parmotremaperlatum.The XRD confirms the formation of CuO with JCPDS NO (01-080-1916) and the crystalline Nature is found as monoclinic phase of end center. Due to Mo doping and lichen extract activity the PCuOM nanoparticle size was much reduced to14 nm.The doping influences the grain shape to irregular rock like structure was formed, as it was confirmed with SEM analysis. The presence of expected elements was confirmed with EDX spectrum. The combined effect of phytochemicals and Mo doping shows higher zone of inhibition against *Bacillus subtilus and Pseudomonas aeruginosa* about 16 mm and 22 mm respectively, when compared to other bacteria.It confirmed that the green PCuOM possessed an improved photocatalytic degradation of Amaranth dye under visible light.The phytochemicals of *parmotremaperlatum* lichen and Mo doping has played major role in structure, morphology antibacterial and photocatalytic activity of CuO nanoparticle.

5.Competing Interest Policy

We, authors have no competing interest

References

1. M. Singh, S. Singh, S. Prasad, I.S. Gambhir, Nanotechnology in medicine and antibacterial effect of silver nanoparticles, Dig. J. Nanomater. Bios. 3 (2008) 115–122.
2. G.M. Whitesides, Nanoscience, nanotechnology and chemistry, Small 1 (2005) 172–179.
3. B. Pelaz, S. Jaber, D.J. De Aberasturi, V. Wulf, T. Aida, J.M. de la Fuente, N. A. Kotov, The state of nanoparticle-based nanoscience and biotechnology: progress, promises and challenges, ACS Nano 6 (2012) 8468–8483, https://doi.org/ 10.1021/nn303929a.
4. C. Jianrong, M. Yuqing, H. Nongyue, W. Xiaohua, L. Sijiao, Nanotechnology and biosensors, Biotechnol. Adv. 22 (2004) 505–518, https://doi.org/10.1016/j. biotechadv.2004.03.004.
5. X. Zhang, Q. Guo, D. Cui, Recent advances in nanotechnology applied to biosensors, Sensors 9 (2009) 1033–1053,
6. B.D. Yao, Y.F. Chan, N. Wang, Formation of ZnO nanostructures by a simple way of thermal evaporation, Appl. Phys. Lett. 81 (2002) 757–759, https://doi.org/ 10.1063/1.1495878.
7. Y. Yin, R.M. Rioux, C.K. Erdonmez, S. Hughes, G.A. Somorjai, A.P. Alivisatos, Formation of hollow nanocrystals through the nanoscale Kirkendall effect, Science 304 (2004) 711–714.
8. J.V. Barth, G. Costantini, K. Kern, Engineering atomic and molecular nanostructures at surfaces, in: Nanoscience and Technology: A Collection of Reviews from Nature Journals, 2010, pp. 67–75.
9. A. Arumugam, C.Karthikeyan, Abdulrahman, S. H. Hameed, K.Gopinath, S.Gowri, Viswanathan, Karthika, Synthesis of cerium oxide nanoparticles using GloriosasuperbaL.leaf extract and their structural, optical and antibacterial properties, *Mater. Sci. Eng. C* 49(1) (2015)408–415.
10. Mie, R., Samsudin, M.W., Din, L.B., Ahmad, A., Ibrahim, N. and Adnan, S.N.A. (2014) Synthesis of Silver Nanoparticles with Antibacterial Activity Using the Lichen Parmotremapraesorediosum. International Journal of Nanomedicine, 9, 121-127. http://doi.org/10.2147/ijn.s52306

11. Hussain, I., Singh, N., Singh, A., Singh, H. and Singh, S. (2016) Green Synthesis of Nanoparticles and Its Potential Application. Biotechnology Letters, 38, 545-560.
12. Kambar, Y., Vivek, M., Manasa, M., Vinayaka, K., Mallikarjun, N. and Kekuda, P.T. (2014) Antimicrobial Activity of Leptogiumburnetiae, Ramalinahossei, Roccellamontagnei and Heterodermiadiademata, International Journal of Pharmaceutical and Phytopharmacological Research, 4, 164-168.
13. Montgomery Maggie A, Elimelech Menachem, Water and sanitation in developing countries: including health in the equation in ACS Publications, 2007.
14. Mittal Alok, MalviyArti, Kaur Dipika, Mittal Jyoti, KurupLisha, Studies on the adsorption kinetics and isotherms for the removal and recovery of Methyl Orange from waste waters using waste materials, Journal of Hazardous Materials, 148 (2007) 229-240.
15. S.M.A, B.P. W, Elimelec Menachem, G.J.G, M.B.J, M.A.M, Science and technology for water purification in the coming decades, Nature, 452 (2008) 301.
16. Gupt Vinod Kumar, Kumar Rajeev, Nayak Arunima, Saleh Tawfi A, Baraka MA, Adsorptive removal of dyes from aqueous solution onto carbon nanotubes: a review, Advances in Colloid and Interface Science, 193 (2013) 24-34.
17. Hammud Hassan H, Shmait Abeer, Hourani Nadim, Removal of malachite green from water using hydrothermally carbonized pine needles, RSC Advances, 5 (2015) 7909-7920.
18. Hariharan C, Photocatalytic degradation of organic contaminants in water by ZnO nanoparticles: Revisited. Applied Catalysis A: General, 2006. **304**: p. 55-61.
19. Gao G, et al., Selectivity of quantum dot sensitized ZnO nanotube arrays for improved photocatalytic activity. Physical Chemistry Chemical Physics, 2017. **19**(18): p. 11366-11372
20. G.K. Weldegebrieal, Photocatalytic and antibacterial activity of CuO nanoparticles biosynthesized using Verbascumthapsus leaves extract, Optik, 204 (2020), 164230.
21. Devasenan S, HajaraBeevi N, Jayanthi S.S, Int. J. of Chem Tech Res., 9 (**2016**) 725-730
22. Kanagasubbulakshmi S and Kadirvelu K, Def. Life Sci. J., 2 (**2017**)422-427.
23. A. Muthuvel, M. Jothibas, C. Manoharan, Synthesis of copper oxide nanoparticles by chemical and biogenic methods: photocatalytic degradation and in vitro antioxidant activity, Nanotechnol. Environ. Eng., 5 (2020), 14

24. Sadia Aroob, M. S. et al. Green synthesis and photocatalytic dye degradation activity of CuO nanoparticles. Catalysis. 13(4), 1–8. https://doi.org/10.3390/catal13030502 (2023).
25. Akintelu S. A, Folorunso A. S, Folorunso, F. A. & Oyebamiji A. K, Green synthesis of copper oxide nanoparticles for biomedical application and environmental remediation. Heliyon. 6(7), e04508. https://doi.org/10.1016/j.heliyon.2020.e04508 (2020).
26. Andualem W. W, Sabir, F. K, Mohammed E. T, Belay H. H. & Gonfa B. A, Synthesis of copper oxide nanoparticles using plant leaf extract of cathaedulis and its antibacterial activity. J. Nanotechnol. https://doi.org/10.1155/2020/2932434 (2020).
27. 35. Alhalili Z, Green synthesis of copper oxide nanoparticles CuO NPs from Eucalyptus Globulus leaf extract: Adsorption and design of experiments. Arab. J. Chem. 15(5), 103739. https://doi.org/10.1016/j.arabjc.2022.103739 (2022)
28. A.C. Nwanya, M.M. Ndipingwi, N. Mayedwa, L.C. Razanamahandry, C.O. Ikpo, T. War yo, S.K.O. Ntwampe, E. Malenga, E. Fosso Kankeu, F.I. Ezema, E.I. Iwuoha, M. Maaza, Maize (Zea mays L.) fresh husk mediated biosynthesis of copper oxides: potentials for pseudo capacitive energy storage, Electrochim. Acta, 301 (2019), pp. 436-448
29. K. Vijai Anand et al., Photocatalytic degradation of rhodamine B dye using biogenic hybrid ZnO-MgO nanocomposites under visible light, Chem. Select 4 (17) (2019) 5178–5184.
30. M.A. Al-Bedairy, H.A.H. Alshamsi, Environmentally friendly preparation of zinc oxide, study catalytic performance of Photodegradation by sunlight for rhodamine B dye, Eurasian J. Anal. Chem. 13 (6) (2018)

Supplementary Files

This is a list of supplementary files associated with this preprint. Click to download.

- SourceDataFig1a1.docx
- SourceDataFig1a2.docx
- SourceDataFig1a3.docx
- SourceDataFig2a.odt
- SourceDataFig2b.docx
- SourceDataFig2c.docx
- SourceDataFig3a.docx
- SourceDataFig3b.docx
- SourceDataFig3c.docx
- SourceDataFig5a.txt
- SourceDataFig5b.txt
- SourceDataFig5c.txt